Study of Matrigel deformation during the formation of 3D tubular networks of intestinal epithelial cells

Author: Alejandro Caro Chacón
Facultat de Física, Universitat de Barcelona, Diagonal 645, 08028 Barcelona, Spain.

Advisor: Jordi Comelles Pujadas

Abstract: Intestinal epithelial cells auto-organize in both three-dimensional (3D) networks and two-dimensional (2D) monolayers depending on the concentration of the extracellular matrix in which they are being grown (Matrigel) causing its deformation. With the use of time lapse videos and fluorescence beads we obtain the velocity fields with a technique called Particle Image Velocimetry. We then use these velocity fields to characterize the rates of deformation with the strain rate tensor. We observe how the magnitudes of the rates of deformation for the high concentration Matrigel are larger than the ones of the low concentration Matrigel which correlates with the observations.

I. INTRODUCTION

The intestinal epithelium is formed by a monolayer of cells called intestinal epithelial cells (IEC). The main function of these cells is to absorb nutrients and protect the body against external threats. IECs *in vivo* are known [1] to form 3D invaginations called crypts and evaginations called villi. (FIG. 1a). In homeostasis, the intestinal epithelial stem cells are located in the crypts, they divide and the daughter cells migrate towards the villus while differentiating. Upon reaching the tip of the villus, these cells are shed off which leads to a completely renewed tissue every 4-5 days. *In vitro*, when IECs are grown they form self-organized 3D structures that recapitulate the *in vivo* architecture called organoids (FIG. 1b). When these organoids grow, they form protruding crypts and in this process the Matrigel gets deformed [1],[2]. If these same cells are grown in a 2D Matrigel we observe a different behavior depending on the concentration of Matrigel. For low concentration Matrigel (3 mg/mL) these organoids become monolayers (FIG. 1c) and if the concentration is high (10 mg/mL) they auto-organize in 3D tubular networks (FIG. 1d) [1],[2],[3]. In both of these processes the Matrigel gets deformed, but in different ways. Previous experiments have shown that in the case of the formation of monolayers the Matrigel is redistributed underneath the cells while in the case of the 3D networks the Matrigel is rearranged all-around of the 3D structure.

To better understand the process of this rearrangement, time-lapse experiments imaging both the cells and the Matrigel were performed. To do so, fluorescence beads were added to the Matrigel in order to have a signature of the dynamics of the matrix. One image was taken every 10 minutes to create the videos of the Matrigel deforming. This deformation has been observed but not quantitatively characterized, so this is the aim of this project. Here, we have studied six individual experiments, three with low concentration Matrigel and three with high concentration Matrigel. We used the strain rate tensor to characterize the deformations and we observed that the magnitude of the rate of deformations for the high concentration Matrigel is about 10 times higher than the magnitude of the low concentration Matrigel.

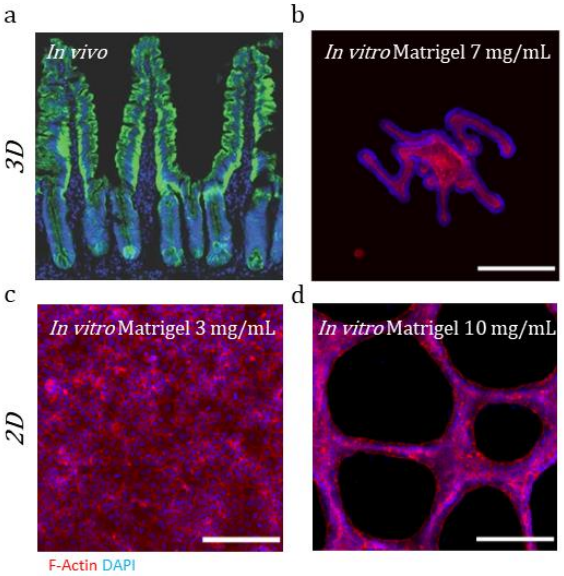

FIG. 1: (a) *In vivo* image the intestinal epithelium. (b) 3D organoid grown *in vitro* in 7 mg/mL concentration Matrigel. (c) Monolayer structures formed in low concentration Matrigel. (d) 3D tubular networks formed in high concentration Matrigel. Scale bars: 200µm. Adapted from [1].

II. METHODS

A. Strain rate tensor

In continuum mechanics the concept of deformation refers to the motion of the particles of a system relative to a given particle [4]. The strain is defined as the variation of the relative position of the particles in the neighbourhood of a given particle. Therefore, the rate of change of this relative position is the strain rate. These concepts can be applied to any continuous medium so there is no restriction using it to describe the deformations of the Matrigel [5]. As we are

working with the variation of positions, we need to use the velocities of each point, so we first need to define the 2D gradient of the velocity:

$$\nabla \boldsymbol{v} = \begin{pmatrix} \frac{\partial v_x}{\partial x} & \frac{\partial v_y}{\partial x} \\ \frac{\partial v_x}{\partial y} & \frac{\partial v_y}{\partial y} \end{pmatrix} \quad (1)$$

The velocity gradient tensor can be split into a symmetric and an antisymmetric matrix:

$$\boldsymbol{E} = \frac{1}{2}(\nabla \boldsymbol{v} + \nabla \boldsymbol{v}^{\boldsymbol{T}}) \quad (2)$$

$$\boldsymbol{R} = \frac{1}{2}(\nabla \boldsymbol{v} - \nabla \boldsymbol{v}^{\boldsymbol{T}}) \quad (3)$$

The symmetric part is called strain rate tensor and it gives us the information about the rate of stretching of the material. On the other hand, the antisymmetric matrix contains the rates of rotation. In a first approach, we have focused on the strain component rather than the rotational component because in the videos of the beads it seems that the stretching of the Matrigel is what makes it deform in the observed manner.

Finally, we can also decompose the strain rate tensor in two components. The first one corresponds to the trace of this tensor and gives us the rate of compression or expansion of the Matrigel around a certain point:

$$\nabla \cdot \boldsymbol{v} = \frac{\partial v_x}{\partial x} + \frac{\partial v_y}{\partial y} \quad (4)$$

If this trace is positive in a certain point, we know that we have a source of material, basically the Matrigel will move away from that point. Likewise, when the trace is negative the point acts as a sink so the Matrigel will tend to accumulate there (FIG. 2a).
The other component is the rate of shear that the Matrigel experiences.

$$\dot{\boldsymbol{\gamma}} = \frac{\partial v_x}{\partial y} + \frac{\partial v_y}{\partial x} \quad (5)$$

This value corresponds to the rate of deformation of the Matrigel produced by shear stress. It makes the material stretch in a certain direction depending on the forces acting (FIG. 2b).

B. Particle Image Velocimetry

To work with the strain-rate tensor, we first need to obtain the velocity field of the Matrigel. To do so, we have used a technique called Particle Image Velocimetry (PIV). This method is based on performing a cross correlation analysis of consecutive images of the beads to compute the velocities of each point. The software used is a MATLAB toolbox called PIVlab [6].

This software subdivides each frame in several interrogation areas (IA) in which it will perform de cross correlation of the beads. To decide the optimal IA size, one

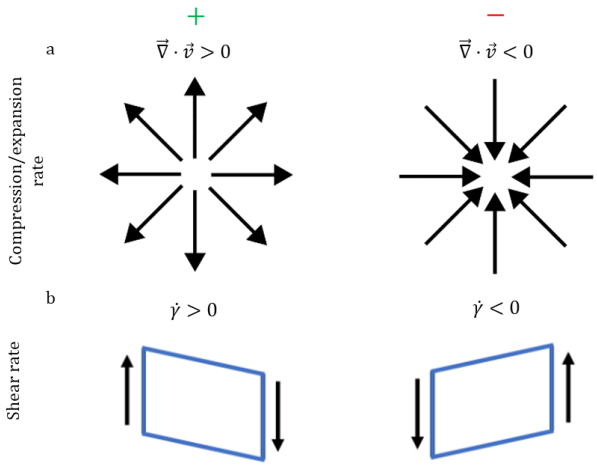

FIG. 2: (a) Sign criteria of the compression and expansion rate. On the left side we have a source so its sign is positive and on the right side there is a sink so its sign is negative. (b) Sign criteria of the shear rate. The positive sign (left) corresponds to a clockwise deformation and the negative (right) one an anticlockwise rotation.

has to be sure that the beads stay in this area for at least a couple of frames so the PIV analysis can be performed properly. We have taken into account the fastest bead of all the experiments and selected the IA such as that bead was several frames inside. Now that we know that this area is enough to track the fastest bead, we also know that the other beads will be inside the area enough time, and then we can use this IA for all the experiments to get the velocity fields.

The images used (FIG 3) are 320 x 320 µm and the analysis consist of two passes of cross-correlation in order to obtain more accurate velocity fields. The first one has an IA of 80µm with a step of 40 µm and the second one is 40 µm with a step of 20 µm. Once we have performed the analysis, we apply a standard deviation filter of 8 standard deviations to the velocities so that we remove any outlier. Finally, we get the mean velocity of all the frames. These mean velocities are the ones used in the analysis of the rates of deformation performed in this experiment because they give us the average behaviour of each point and it correlates properly with the video of the beads.

C. Correlation length

The correlation function measures the order of a system and it helps us to see how different variables are correlated between them. With the correlation function we can see how these variables co-vary on average in time and space. The definition of this function between two variables x and y is the following:

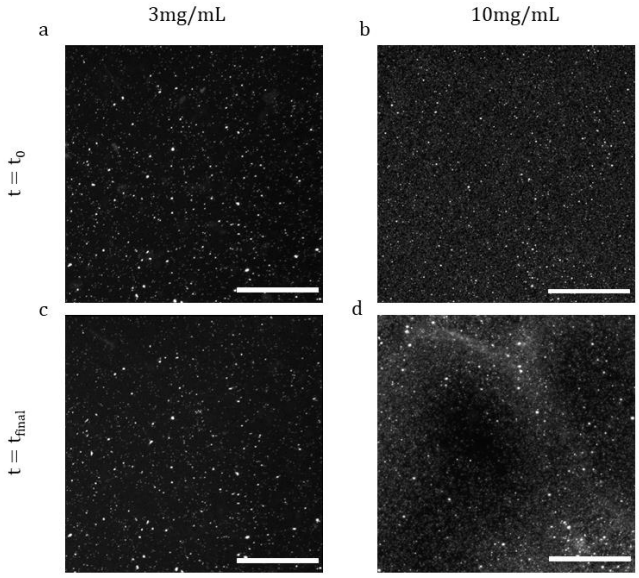

FIG. 3: (a) First frame of one of the experiments with low concentration Matrigel. (b) First frame of one of the experiments of high concentration Matrigel. (c) Last frame of the same low concentration Matrigel. There is no apparent movement between the first and last frames. (d) Last frame of the same high concentration Matrigel. We can see the rearrangement of the Matrigel. Scale bars: 100μm.

$$C(\delta\vec{r},\delta t) = \langle x(\vec{r},t)\cdot y(\vec{r}+\delta\vec{r},t+\delta t)\rangle - \langle x(\vec{r},t)\rangle\langle y(\vec{r}+\delta\vec{r},t+\delta t)\rangle \quad (6)$$

As we have the velocity fields of the Matrigel we will work with the velovity-velocity correlation function [7] to see how these velocities correlate to each other. In a first approach, we will only compute the correlation depending on the distance between points, so we will only work with the mean of the velocities and ignore the temporal part.

$$C(\delta\vec{r}) = \frac{\langle\vec{v}(\vec{r}+\delta\vec{r})\cdot\vec{v}(\vec{r})\rangle}{\langle v(\vec{r})^2\rangle} \quad (7)$$

Once we have this correlation for every distance $\delta\vec{r}$, we can compare how fast the correlation disappears based on the distance to a certain point. From this correlation function we are going to define the correlation length as the distance where the correlation goes under 25%.

III. RESULTS

The first thing we observe when comparing the results from the PIV analysis is the difference in the velocity fields produced by the different concentration of Matrigel. Figure 4a corresponds to the velocity field of the 3 mg/mL concentration Matrigel and we observe velocities of low magnitude with no preferential direction. The velocity field of the 10 mg/mL Matrigel (FIG. 4b) shows domains with well-defined direction of movement and the magnitude of these velocities is larger than in the 3mg/mL experiment.

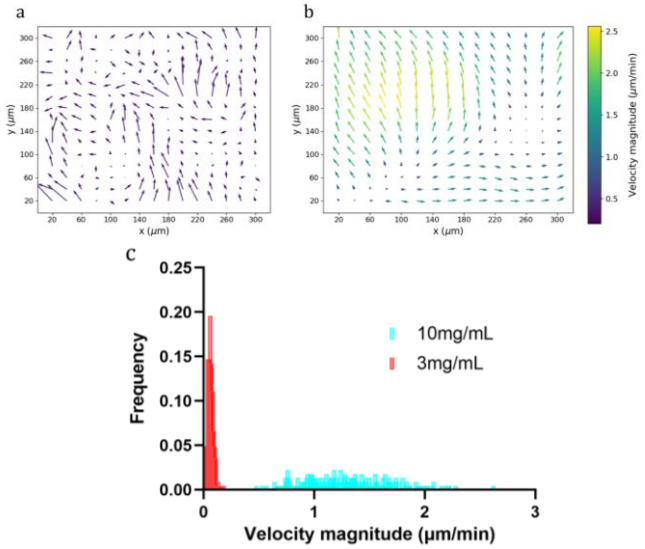

FIG. 4: (a) Velocity field of the low concentration Matrigel. (b) Velocity field of the high concentration Matrigel. (c) Histogram of the velocities of each Matrigel concentration. The low concentration Matrigel only has low velocities compared to the high concentration one so we see a high frequency of values around 0. The velocities of the 10 mg/mL Matrigel are more spread out so their relative frequency is lower.

When we compare the magnitude of the velocities of all the experiments at once (FIG. 4c) we can clearly see how the velocities of the low concentration Matrigel are close to 0μm/min while the velocities of the high concentration Matrigel are more than 10 times larger, reaching about 2μm/min. This is to be expected because we see few movement of the beads in the videos for low concentration Matrigel, while beads on high Matrigel concentration are displaced large distances. Altogether, we can see how the average velocities are much higher for the high concentration Matrigel and how the velocity field shows a clear direction of displacement compared with the low concentration Matrigel.

For the compression/expansion rate we also see differences in magnitude between the two types of Matrigel. We can see how the low concentration Matrigel (FIG. 5a) has almost no expansion or compression, we only see a flat heat map with very low rates of deformation. For instance, the high concentration Matrigel (FIG. 5b) shows clear patterns of rates of deformation. This is to be expected as the beads in the 3 mg/mL Matrigel move in a random way without any particular direction, therefore the deformation averages out. On the contrary, the more coherent move of the beads in 10 mg/mL leads to clear deformation patterns. The areas where we have positive values correspond to the holes that we see being created in the Matrigel as the beads go away. If we compare these patterns to the final frame of the experiment (FIG. 3d) we can see how they correlate to the structures formed by the Matrigel.

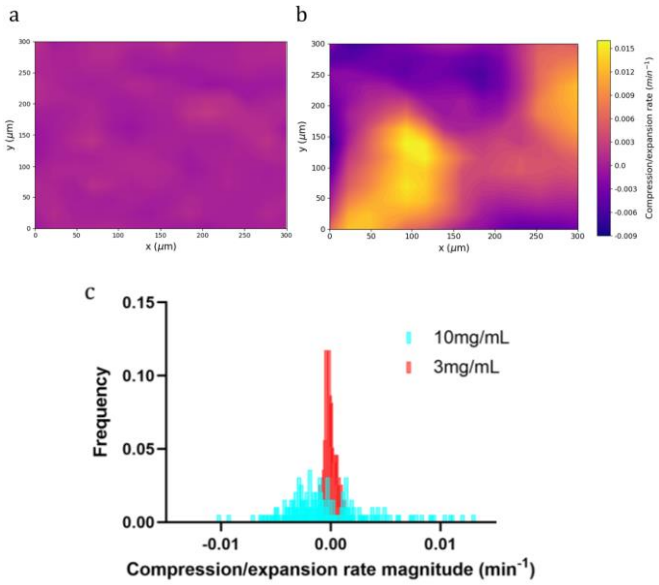

FIG. 5: (a) Heat map of the compression or expansion rate for the low concentration Matrigel. The scale is normalized to the high concentration Matrigel. (b) Heat map of the compression or expansion rate for the high concentration Matrigel. (c) Histogram of the rate of compression/expansion for all the experiments.

If we now compare all the experiments at once (FIG. 5c) we see once again how the magnitude of the rate of compression/expansion of the high concentration Matrigel is larger than the low concentration Matrigel. We can also see how the rates of compression/expansion of the 10 mg/mL Matrigel is displaced slightly towards the negative values. That means that these experiments have an overall tendency of acting as a material sink so the beads from outside the field of view tend to go inside it. This has no further importance and it is caused by the low number of experiments available to analyse. Given enough samples or larger fields of view we should see how the distribution becomes symmetrical and centered around 0. Basically, we observe how the magnitude of the rate of compression/expansion is a couple times larger in the high concentration Matrigel and this rate of compression/expansion correlates with the structures formed by the Matrigel.

The shear rate presents a similar behaviour as the compression/expansion rate. The 3 mg/mL Matrigel presents almost no deformation (FIG. 6a) when compared with the 10 mg/mL one. The high concentration Matrigel presents different values for the shear rate (FIG. 6b), about a couple times larger than the low concentration one. In this case the correlation with the structures seen in the videos is not as clear so the shear rate will not help us to correlate the rates of deformation with the videos.

When we compare the shear rate of all the experiments at once (FIG. 6c), we see again a similar distribution as the compression/expansion rate. The values of the low concentration Matrigel are located very close to 0 and the values of the high concentration Matrigel are more spread out. Altogether we can see how the difference in magnitude of the rates of shear is quantitatively different between concentrations of Matrigel and how in this case these rates don't really correlate to the structures formed by the Matrigel as clear as the compression/expansion rates.

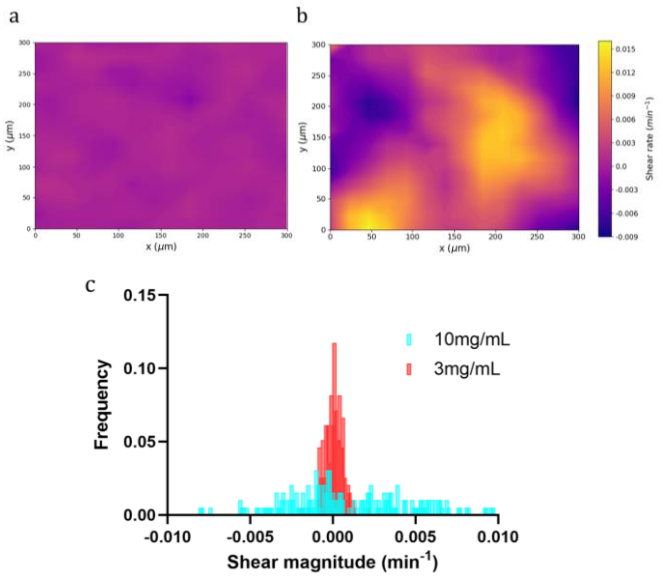

FIG. 6: (a) Heat map of the shear rate for the low concentration Matrigel. The scale is normalized to the high concentration Matrigel. (b) Heat map of the shear rate for the high concentration Matrigel. (c) Histogram of the rate of shear for all the experiments.

Lastly, we have studied how correlated are the velocities of each experiment based on the distance of a certain point. As we expected we observe how the correlation decreases as the distance grows and how the correlation on the low concentration Matrigel falls faster than the correlation on the high concentration Matrigel (FIG. 7a). In the low concentration Matrigel this correlation decreases faster because the Matrigel does not deform in a uniform manner so there is not that much correlation between points that are far away. On the contrary, in the high concentration Matrigel we can see how certain regions are displaced in a uniform manner so these velocities would have more correlation even if we are farther away. It is important to note how the correlation never goes to 0. This may be caused by the fact that cellular structures (either monolayers or tubular networks) are connected to the Matrigel, thus conferring to the material a certain 'long-range' structure.

If we now compare the values of the correlation length (TABLE I) we see how the correlation length of the 10 mg/mL Matrigel is almost three times the one of the 3 mg/mL. It is also very interesting to see how the correlation length is very similar to the size of the structures on the Matrigel (FIG. 7b). We can observe this for the high concentration Matrigel but not for the low concentration one because this one doesn't create any structures so this correlation length is not really that useful for this case.

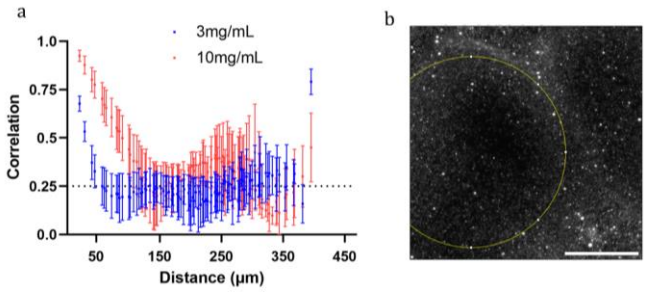

FIG. 7: (a) Correlation depending on the distance of low concentration Matrigel (blue) and high concentration Matrigel (red). The dotted line represents a correlation of 0.25. (b) Circle with the correlation length of the high concentration Matrigel as radius. Scale bar: 100µm.

To actually see if the correlation length is useful to describe the characteristic size of the structures, we would need to increase the area studied to have several structures inside the image because in the size of the window of this experiment only parts of the structures fit so it is hard to analyse this correlation. Interestingly, the correlation length of monolayers was about two to three cells sizes [7], which in our case should correspond to about 36µm. So, while the correlation observed in low concentration Matrigel could correspond to the actual correlation of the cells, in the case of high concentration Matrigel could be linked to a correlation length intrinsic of the material.

	3 mg/mL	10 mg/mL
Correlation length (µm)	54±8	131±4

TABLE I: Correlation length for both concentrations Matrigel.

IV. CONCLUSIONS

In this work we have characterized the different deformations produced by intestinal epithelial cells depending on the concentration of Matrigel. We have found that the magnitude of the velocity field for the high concentration Matrigel is ten times larger than the low concentration Matrigel. Analogously, the magnitude of the compression/expansion rate for the low concentration Matrigel is almost negligible compared with the magnitude of the high concentration one and correlates with the structures formed by the Matrigel. On the contrary, the shear rate does not match the high concentration Matrigel patterns, despite also being significantly higher than the low concentration Matrigel. Finally, the correlation length is about three times larger in the high concentration Matrigel as we see a faster decrease in the correlation of the velocities for the low concentration Matrigel.

Acknowledgments

First of all, I want to thank my advisor Jordi Comelles for all the help and guidance provided to complete this work. I would also like to thank all the members of the Biomimetic Systems for Cell Engineering for allowing me to be part of their team during all these months. Finally, without my family I wouldn't be here today so thanks for all your support.

[1] E. Larrañaga, "Effects of substrate-derived cues in driving the self-organization of organoid-derived intestinal epithelia," Ph.D. dissertation, Dept. Biomed. Eng., Universitat de Barcelona, Spain, 2021

[2] C. Davidson et al, "Cell force-mediated matrix reorganization underlies multicellular network assembly," *Scientific Reports*, vol. 9, issue 1, p. 12, 2019.

[3] D. Rüdiger et al, "Cell-Based Strain Remodeling of a Nonfibrous Matrix as an Organizing Principle for Vasculogenesis," *Cell Reports*, vol. 32, issue 6, p. 108015, 2020.

[4] X. Oliver and C. Agelet de Saracibar, *Continuum Mechanics for Engineers. Theory and Problems*, 2nd ed. 2017.

[5] P. Sanematsu et al, "3D viscoelastic drag forces contribute to cell shape changes during organogenesis in the zebrafish embryo," *Cells & Development*, vol. 168, p. 203718,, 2021.

[6] W. Thielicke and R. Sonntag, "Particle Image Velocimetry for MATLAB: Accuracy and enhanced algorithms in PIVlab," *Journal of Open Research Software*, vol. 9, issue 1, p. 12, 2021.

[7] S. Garcia et al, "Physics of active jamming during collective cellular motion in a monolayer," *Proceedings of the National Academy of Sciences*, vol. 112, issue 50, pp. 15314-15319, 2015.